SOLVING WAVE EQUATIONS IN THE CURVELET DOMAIN: A MULTI-SCALE AND MULTI-DIRECTIONAL APPROACH

BINGBING SUN[1], JIANWEI MA[1,2], HERVÉ CHAURIS[2] and HUIZHU YANG[1]

[1] *Institute of Seismic Exploration, School of Aerospace, Tsinghua University, P.R. China.*
[2] *Centre de Géosciences, Mines ParisTech, Paris, France. herve.chauris@mines-paristech.fr*

(Received April 15, 2009; revised version accepted June 15, 2009)

ABSTRACT

Sun, B., Ma, J., Chauris, H. and Yang, H., 2009. Solving wave equations in the curvelet domain: a multi-scale and multi-directional approach. *Journal of Seismic Exploration*, 18: 385-399.

Seismic imaging is a key step in seismic exploration to retrieve the earth properties from seismic measurements at the surface. One needs to properly model the response of the earth by solving the wave equation. We present how curvelets can be used in that respect. Curvelets can be seen from the geophysical point of view as the representation of local plane waves. The unknown pressure, solution of the wave equation, is decomposed in the curvelet domain. We derive the new associated equation for the curvelet coefficients and show how to solve it. In this paper, we focus on a simple homogeneous model to illustrate the feasibility of the curvelet-based method. This is a first step towards the modeling in more complex models. In particular, we express the derivative of the wave field in the curvelet domain. The simulation results show that our algorithm can give a multi-scale and multi-directional view of the wave propagation. A potential application is to model the wave motion in some specific directions. We also discuss the current limitations of this approach, in particular the extension to more complex models.

KEYWORDS: curvelets, wavelets, numerical simulation, wave equation, multi-scale, multi-directional, adaptive.

INTRODUCTION

In the context of seismic oil and gas exploration, numerical simulation of the wave equation is the key factor to establish the link between the earth properties and the observed data at the surface. Among several traditional methods for the wave field simulation, the finite difference method (Alford et al., 1974; Alterman and Karal, 1968; Kelly et al., 1976) is the most popular.

0963-0651/09/$5.00

It uses values on several grid points to estimate the derivative at a particular location. Its advantage relies on the relatively easy programming and high speed calculation. The pseudospectral method (Fornberg, 1989; Gazdag, 1981; Kosloff and Baysal, 1982) have also been proved to be an efficient method. Compared to low-order finite difference, the pseudospectral method provides more accurate result as it uses all grid point values to estimate the derivatives. Beyond these two methods, the finite element method (Lysmer and Draker, 1972; Meyer, 1992) is based on the variational principle while the boundary element method (Carrer et al., 2008; Funato and Fukui, 1999) is based on the integral principle. Both methods have good performance in stability and convergence, and can deal with complicated boundary conditions. However, these two methods are generally memory- and time-consuming.

In the past, the mentioned methods have been improved in terms of speed and accuracy. We focus here on a different aspect, related to multi-scale and multi-direction analysis. Wavelet schemes (Carrer et al., 2008; Kelly et al., 1976) provide a multi-scale solution where the basis elements are relatively well localized in the time and frequency domains, with a large number of applications in data processing (Antoine et al., 2004; Daubechies, 1992). Combined with other methods, wavelets can be used to solve the wave equation (Hong and Kennett, 2002a; Hong and Kennett, 2002b; Ma et al., 2001). The numerical algorithms have a number of advantages: the differential operator can be directly computed in the wavelet domain with high speed and accuracy; by setting threshold values in the wavelet domain, significant coefficients can be selected to reduce the calculations and the memory requirement; it is also possible to derive the wave field corresponding to certain scales without calculating the whole wave field.

Compared to wavelets, curvelets appears to be more suitable for solving hyperbolic problems (Candès and Demanet, 2005; Candès and Donoho, 2003). Curvelets (Candès and Donoho, 2000, 2004, 2005) were recently introduced in the field of applied harmonic analysis and have a number of applications on seismic processing (Lin and Herrmann, 2007; Herrmann et al., 2008; Ma et al., 2007; Ma and Plonka, 2009a, 2009b). They provide a multi-direction analysis and allow a sparse representation of smooth objects containing smooth discontinuities (i.e., twice continuously differentiable). Curvelets preserve the same time-frequency localization property as for wavelets and at the same time, with their elongated support in the Fourier domain, curvelets become directional.

Compared to the Fourier and wavelet analysis, the curvelet decomposition (Candès and Demanet, 2005; Candès and Donobo, 2003) theoretically provides an optimally sparse representation of the wave propagator. For example, Demanet (2006) uses curvelet-like wave atoms to solve the wave equation. His

algorithm is based on the sparsity of the matrix representation of Green's function. In his paper, the curvelets are used as basic functions and the derivatives are calculated through them. Because of lack of explicit expressions of the curvelets in the time domain, the derivative is computed numerically in the frequency domain, raising the computation aspect. Andersson et al. (2008) developed a method based on the Volterra equation (high frequency approximation) and considers the rigid motion of the curvelet along the ray. The wave operator is decomposed into individual scale using para-differential decomposition. The Hamilton flow at a given scale determines the motion of the curvelets. As for curvelet-based migration (Chauris and Nguyen, 2008; Douma and de Hoop, 2007), that focuses on the action of the migration operator on the curvelets, only the first-order approximation of the distorted curvelet is predicted. Moreover, the location of the discrete curvelets is not necessarily on the original grid, requiring some interpolation procedure (Chauris and Nguyen, 2008). Ma et al. (2007) introduced the curvelet transform into AMR (adaptive mesh refinement) to estimate the local error of the wave field so as to update the grid. This method suffers from the lack of analytical expression in space of the current curvelet transform.

In order to get a multi-scale and multi-direction analysis of the wave propagation, and for calculation efficiency, we solve the wave equation directly in the curvelet coefficient domain. In this paper, we show how to express the derivative of a function in the curvelet domain. The curvelet decomposition is coupled to the Finite Difference scheme, providing a multi-scale and multi-direction analysis of the wave field.

The outline of the paper is as follows. First, we explain the curvelet construction and the main properties of curvelets. Then, we show how to solve the wave equation in the curvelet domain for homogeneous models, including numerical examples. Finally, we discuss the current limitations of the approach.

CURVELETS

In this section, we give a brief introduction of the curvelet transform. First we define the continuous curvelet transform (Candes and Donoho, 2004; Candes et al., 2005).

In the two-dimensional space R^2, define the spatial variable $x = (x_1,x_2)$ and its counterpart $\omega = (\omega_1,\omega_2)$ in the frequency domain or alternatively the polar coordinates $r = \sqrt{(\omega_1^2 + \omega_2^2)}$ and $\theta = \arctan(\omega_2/\omega_1)$. We first start with a pair of window functions $W(r)$ and $V(t)$, called the "radial window" and "angular window". These window functions are both smooth, non-negative and real-valued, with W taking positive real arguments and supported on $r \in (1/2,2)$ and V taking real arguments and supported on $t \in [-1,1]$. Both obey

the admissibility conditions:

$$\sum_{j=-\infty}^{\infty} W^2(2^j r) = 1, r \in (3/4,3/2) \quad , \tag{1}$$

$$\sum_{l=-\infty}^{\infty} V^2(t - l) = 1, t \in (-1/2,1/2) \quad . \tag{2}$$

For $j \geq j_0$, we define the filter U_j in the frequency domain by

$$U_j(r,\theta) = 2^{-3j/4} W(2^{-j} r) V(2^{[j/2]}\theta/2\pi) \quad , \tag{3}$$

where [j/2] denotes the integer part of j/2. The support of U_j is a polar "wedge".

The waveform $\varphi_j(x)$ is defined by its Fourier transform $\hat{\varphi}_j(\omega) = U_j(\omega)$ where $U_j(\omega)$ is defined in the polar coordinate system by eq. (3). All the curvelets at scale 2^{-j} are obtained by rotations and translations of φ_j. Given the equispaced sequence of rotation angles $\theta_l = 2\pi \cdot 2^{-[j/2]} \cdot l$, with $l = 0,1,\ldots 2^{[j/2]}$, so $0 \leq \theta_l \leq 2\pi$ and the sequence of translation parameters $k = (k_1,k_2) \in Z^2$. Note the spacing between angles is scale-dependent. We define curvelets at scale 2^{-j}, orientation θ_l, and position $x_k^{(j,l)} = R^{-} (k_1 \cdot 2^{-j}, k_2 \cdot 2^{-j/2})$ [Let b denote $(k_1 \cdot 2^{-j}, k_2 \cdot 2^{-j/2})$].

$$\varphi_{j,l,k}(x) = \varphi_j[R_{\theta_l}(x - x_k^{(j,l)})] = \varphi_j(R_{\theta_l} x - b) \quad , \tag{4}$$

where R_{θ_l} is the rotation by θ_l radians and $R_{\theta_l}^{-}$ its inverse,

$$R_{\theta_l} = \begin{pmatrix} \cos\theta_l & \sin\theta_l \\ -\sin\theta_l & \cos\theta_l \end{pmatrix} \quad . \quad R_{\theta_l}^{-} = R_{\theta_l}^{T} = R_{-\theta_l} \tag{5}$$

The curvelet family forms a tight frames: we can expand a function $f \in L^2(R^2)$ as a series of curvelets:

$$f = \sum_{j,l,k} \langle f, \varphi_{j,l,k} \rangle \varphi_{j,l,k} \quad , \tag{6}$$

where $C_{j,l,k}$ denotes the curvelet coefficient or scalar product $\langle f, \varphi_{j,l,k} \rangle$

$$C_{j,l,k} = <f,\varphi_{j,l,k}> = \int_{R^2} f(x)\overline{\varphi_{j,l,k}(x)}dx \quad , \tag{7}$$

According to the Plancherel's theorem, we can express the inner product as the integral over the frequency domain.

$$C_{j,l,k} = [1/(2\pi)^2] \int \hat{f}(\omega)\overline{\hat{\varphi}_{j,l,k}(\omega)}d\omega$$

$$= [1/(2\pi)^2] \int \hat{f}(\omega)U_j(R_{\theta_l}\omega)e^{i<x_k^{(j,l)},\omega>} d\omega \quad . \tag{8}$$

The phase shift in the frequency domain corresponds to a shift in the spatial domain. We introduce the low-pass window W_0 obeying

$$|W_0|^2 + \sum_{j>j_0} |W(2^{-j}r)|^2 = 1 \quad , \tag{9}$$

and define coarse scale curvelets as

$$\varphi_{j_0,k}(x) = \varphi_{j_0}(x - 2^{-j_0}k) \quad , \tag{10}$$

$$\hat{\varphi}_{j_0}(\omega) = 2^{-j_0}(2^{-j_0}|\omega|) \quad . \tag{11}$$

The curvelets associated to the coarse scale curvelets are non directional. The curvelet transform consists of two parts: the fine scale directional elements $(\varphi_{j,l,k})_{j>j_0,l,k}$, the coarse scale isotropic curvelets $(\varphi_{j_0,k})_k$.

At least two existing codes are available (Candes et al., 2005; Ma et al., 2007) for practical applications, respectively based on the USFFT and wrapping. We introduce the USFFT. In the continuous-time definition, the window U_j is defined over the dyadic corona $\{2^j \leq r \leq 2^{j+1}\}$ and the angle $\{-\pi\cdot 2^{-j/2} \leq \theta \leq \pi\cdot 2^{-j/2}$. These are not especially well-suited for Cartesian arrays. We introduce the equivalents: "Cartesian coronae" based on concentric squares, instead of circles, and shears instead of rotations.

The Cartesian analog to the "radial window $(W_j)_{j\geq 0}$, would be a window of the form

$$\tilde{W}_j(\omega) = \sqrt{(\Phi_{j+1}^2 - \Phi_j^2)} \quad , \tag{12}$$

where Φ is defined as the product of low-pass one dimensional windows

$$\Phi_j(\omega) = \phi(2^{-j}\omega_1)\phi(2^{-j}\omega_2) \quad . \tag{13}$$

The function ϕ obeys $0 \leq \phi \leq 1$, might be equal to 1 on $[-1/2,1/2]$, and vanishes outside of $[-2,2]$. One can check that

$$\Phi_0(\omega)^2 + \sum_{j>0} \tilde{W}_j^2(\omega) = 1 \quad . \tag{14}$$

The V_j functions are defined as

$$V_j(\omega) = V(2^{[j/2]}\omega_2/\omega_1) \quad . \tag{15}$$

We can define the "Cartesian" frequency window:

$$\tilde{U}_j(\omega) = \tilde{W}_j(\omega)V_j(\omega) \quad . \tag{16}$$

It is clear that $\tilde{U}_j$ isolates frequency near the wedge $\{(\omega_1,\omega_2) : 2^j \leq \omega_1 \leq 2^{j+1}, -2^{-j/2} \leq \omega_2/\omega_1 \leq 2^{-j/2}\}$. We introduce the equispaced slopes $\tan\theta_l = l\cdot 2^{[-j/2]}$, $l = -2^{j/2},\ldots,2^{[j/2]} - 1,2^{[j/2]}$, and define

$$\tilde{U}_{j,l}(\omega) = \tilde{W}_j(\omega)V_j(S_{\theta_l}\omega) \quad , \tag{17}$$

where S_{θ_l} is the shear matrix,

$$S_{\theta_l} = \begin{pmatrix} 1 & 0 \\ -\tan\theta_l & 1 \end{pmatrix} \quad . \tag{18}$$

The angles θ_l are not equispaced here but the slopes are. After completion by symmetry around the origin and rotation by $\pm\pi/2$ radians, the $\tilde{U}_{j,l}$ define the Cartesian analog to the family $U_j(R_{\theta_l}\omega)$ as mentioned before. The digital coronization suggests Cartesion curvelets of the form

$$\tilde{\varphi}_{j,l,k}(x) = 2^{3j/4}\tilde{\varphi}_j[S_{\theta_l}(x - S_{\theta_l}^{-}b)] \quad ,$$

where b takes on the discrete values $b = (b_1,b_2) = (k_1\cdot 2^{-j},k_2\cdot 2^{-j/2})$. The new expression of the curvelet coefficient is

$$C_{j,l,k} = \int \hat{f}(\omega)\tilde{U}_j(S_{\theta_l}\omega)e^{i<S_{\theta_l}^{-}b,\omega>}d\omega \quad , \tag{19}$$

$$= \int \hat{f}(S_{\theta_l}\omega)\tilde{U}_j(\omega)e^{i<b,\omega>}d\omega \quad . \tag{20}$$

For a discretized version of f on a Cartesian array $f[t_1,t_2], 0 \le t_1,t_2 < n$, where $\hat{f}[n_1,n_2]$ denotes its 2D discrete Fourier transform

$$\hat{f}[n_1,n_2] = \sum_{t_1,t_2=0}^{n-1} f[t_1,t_2]e^{-i2\pi(n_1t_1 + n_2t_2)/n} \quad , \quad -n/2 \le n_1,n_2 < n/2 \tag{21}$$

where $\hat{f}[n_1,n_2] = \hat{f}(2\pi n_1, 2\pi n_2)$. Assume that $\tilde{U}_j[n_1,n_2]$ is supported on some rectangle of length $L_{1,j}$ and width $L_{2,j}$

$$\mathcal{P}_j = \{(n_1,n_2): n_{1,0} \le n_1 < n_{1,0} + L_{1,j}, n_{2,0} \le n_2 < n_{2,0} + L_{2,j}\} \quad , \tag{23}$$

where $(n_{1,0},n_{2,0})$ is the index of the pixel at the bottom-left of the rectangle. Because of the parabolic scaling, $L_{1,j}$ is bout 2^j and $L_{2,j}$ is about $2^{j/2}$. With these notations, the Fast Discrete Curvelet Transform (FDCT) via USFFT evaluates

$$C_{j,l,k} = \sum_{n_1,n_2 \in \mathcal{P}_j} \hat{f}[n_1, n_2 - n_1\tan\theta_l]\tilde{U}_j[n_1,n_2]e^{i2\pi(k_1n_1/L_{1,j} + k_2n_2/L_{2,j})} \quad , \tag{24}$$

We summarize the FDCT via USFFT as follows:

1. Apply the 2D FFT and obtain Fourier samples $\hat{f}[n_1,n_2]$, $-n/2 \le n_1,n_2 < n/2$.

2. For each scale and angle pair (j,l), resample (or interpolate) to obtain sampled values $\hat{f}[n_1, n_2 - n_1\tan\theta_l]$ for $n_1,n_2 \in \mathcal{P}_j$.

3. Multiply the interpolated object $\hat{f}$ with the parabolic window $\tilde{U}_j$, obtain $\hat{f}_{j,l}[n_1,n_2] = \hat{f}[n_1, n_2 - n_1\tan\theta_l]\tilde{U}_j[n_1,n_2])$.

4. Apply the inverse 2D FFT to each $\hat{f}_{j,l}$ to get the discrete coefficients $C_{j,l,k}$.

Fig. 1 gives the spatial and frequency view of a specific curvelet. Ma and Plonka (2007) presented a periodic curvelet transform. For more details on curvelets and recent applications, we refer to reviewal papers (Ma and Plonka, 2009a, 2009b).

SOLVING THE WAVE EQUATION IN THE CURVELET DOMAIN

The main objective is to solve the wave equation in the curvelet domain. The simplest form corresponds to the 2D constant density scalar wave equation.

$$\partial^2u(t,x)\partial/t^2 = a^2\Delta u(t,x), \quad u(t,x)\big|_{t=0} = u_1(x), \quad \partial u(t,x)/\partial t\big|_{t=0} = u_2(x), \tag{25}$$

where u(x,t) is the pressure field, a is the constant wave speed, x denotes (x_1,x_2), and Δ, the Laplace operator $(\partial^2/\partial x_1^2) + (\partial^2/\partial x_2^2)$. We give a detailed description of our new method. It is based on the transposition of the finite difference method in the curvelet domain. We first address how to estimate the spatial derivatives, specifically the Laplacian acting on the pressure u. Our ideas are inspired by the pseudospectral method that establishes a relationship between the Fourier transform of a function and its derivatives. We derive a similar relationship, leading to a new expression of the wave equation in the curvelet domain in the case of homogeneous models. Let us define the curvelet functions in the frequency domain $\hat{\varphi}_{j,l,k}(\omega)$ as

$$\hat{\varphi}_{j,l,k}(\omega) = \tilde{U}_j(S_{\theta_l}\omega)e^{i<S_{\theta_l}b,\omega>} \quad . \tag{26}$$

By construction, the curvelet coefficients associated to u or to its Laplacian are defined by

$$C_{j,l,k} = [1/(2\pi)^2] \int \hat{u}(\omega)\overline{\hat{\varphi}_{j,l,k}(\omega)}\, d\omega \quad , \tag{27}$$

$$C^{\Delta}_{j,l,k} = [1/(2\pi)^2] \int FT(\Delta u)\overline{\hat{\varphi}_{j,l,k}(\omega)}\, d\omega \quad . \tag{28}$$

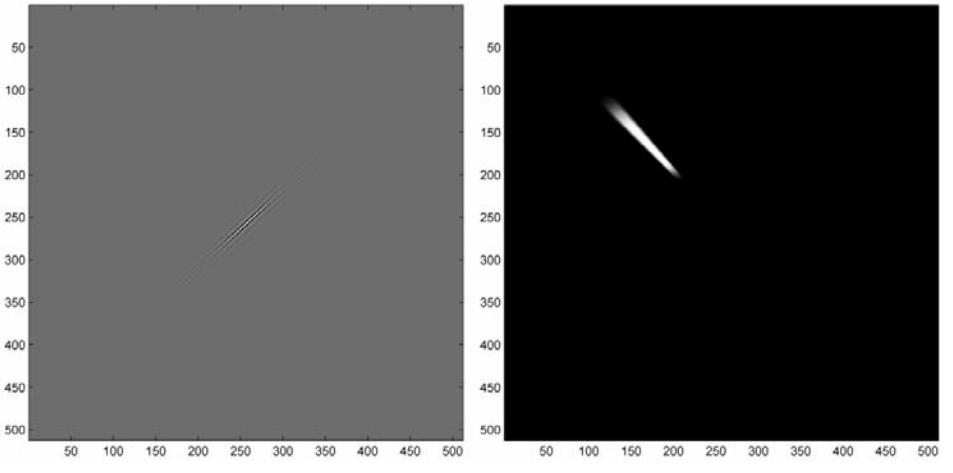

Fig. 1. Spatial and frequency view of a curvelet.

The basic properties of the Fourier Transform (FT) about the derivative give

$$FT(\partial^n f/\partial t^n) = (i\omega)^n \hat{f}(\omega) \quad , \tag{29}$$

so that

$$C^{\Delta}_{j,l,k} = -[1/(2\pi)^2] \int |\omega|^2 \hat{u}(\omega)\overline{\hat{\varphi}_{j,l,k}(\omega)}\, d\omega \quad . \tag{30}$$

We exploit the specific form for $\hat{\varphi}_{j,l,k}$ and perform a change of variables from S ω to ω, yielding to

$$C_{j,l,k} = [1/(2\pi)^2] \int S^{-}_{\theta_l} \hat{u}(\omega)\tilde{U}_j(\omega)e^{i<b,\omega>}\, d\omega \quad , \tag{31}$$

$$C^{\Delta}_{j,l,k} = -[1/(2\pi)^2] \int |S^{-}_{\theta_l}(\omega)|^2 \cdot S^{-}_{\theta_l} \hat{u}(\omega)\tilde{U}_j(\omega)e^{i<b,\omega>}\, d\omega \quad , \tag{32}$$

$$= -[1/(2\pi)^2] \int (\omega_1^2/\cos^2\theta_l + \omega_2^2 - 2\omega_1\omega_2 \tan_{\theta_l}) \cdot S^{-}_{\theta_l} \hat{u}(\omega)\tilde{U}_j(\omega)e^{i<b,\omega>} d\omega \, . \tag{33}$$

We observe that $C^{\Delta}_{j,l,k}$ is composed of three parts, $C^{\Delta}_{k_1}$, $C^{\Delta}_{k_2}$, $C^{\Delta}_{k_1k_2}$:

$$C^{\Delta}_{k_1} = [1/(2\pi\cos\theta_l)^2] \int -\omega_1^2 \tilde{u}(\omega)e^{i<b,\omega>} d\omega \quad , \tag{34}$$

$$C^{\Delta}_{k_2} = [1/(2\pi)^2] \int -\omega_2^2 \tilde{u}(\omega)e^{i<b,\omega>} d\omega \quad , \tag{35}$$

$$C^{\Delta}_{k_1k_2} = [2\tan\theta_l/(2\pi)^2] \int \omega_1\omega_2 \tilde{u}(\omega)e^{i<b,\omega>} d\omega \quad . \tag{36}$$

Consider eq. (34), the integral part can be seen as the inverse Fourier transform of $-\omega_1^2\tilde{u}(\omega)$. We thus obtain

$$C^{\Delta}_{k_1} = (1/\cos^2\theta_l)(\partial^2 C_{j,l,k}/\partial b_1^2) \quad , \tag{37}$$

$$C^{\Delta}_{k_2} = \partial^2 C_{j,l,k}/\partial b_2^2 \quad , \tag{38}$$

$$C^{\Delta}_{k_1k_2} = -2\tan\theta_l (\partial^2 C_{j,l,k}/\partial b_1 \partial b_2) \quad . \tag{39}$$

We now get an expression for the wave equation in the curvelet domain

$$\partial^2 C_{j,l,k}/\partial t^2 = a^2[(1/\cos^2\theta_l)(\partial^2 C_{j,l,k}/\partial b_1^2) + (\partial^2 C_{j,l,k}/\partial b_2^2) - 2\tan\theta_l(\partial^2 C_{j,l,k}/\partial b_1 \partial b_2)] \, . \tag{40}$$

We can use the central difference method or pseudo-spectrum method to

calculate the coefficients. Of course, any efficient methods for solving partial differential equations can be used theoretically.

NUMERICAL SIMULATION AND DISCUSSION

In this section, we present the numerical simulation in an homogeneous velocity model. We include a source term $p(x,t) = \delta(x - x_0)f(t)$ where f is a Ricker wavelet.

$$\partial^2 u/\partial t^2 = a^2[(\partial^2 u/\partial x_1^2) + (\partial^2 u/\partial x_2^2)] + p(x,t) \quad , \tag{41}$$

$$u(t,x)\big|_{t=0} = u_1(x), \quad \partial u(t,x)/\partial t\big|_{t=0} = u_2(x).$$

The complete form of the wave equation in the curvelet domain is given by

$$\partial^2 C_{j,l,k}/\partial t^2 = a^2[(1 + \tan^2\theta_l)(\partial^2 C_{j,l,k}/\partial b_1^2) + (\partial^2 C_{j,l,k}/\partial b_2^2) - 2\tan\theta_l(\partial^2/C_{j,l,k}/\partial b_1 \partial b_2)] + C^{\delta}_{j,l,k} f(t) \quad , \tag{42}$$

where $C^{\delta}_{j,l,k}$ denotes the curvelet transform of function $\delta(x - x_0)$.

We use explicit finite difference method and pseudospectral method to solve eq. (42). The calculation process is as follows:

1. Select the number of scales and directions used in curvelet transform and accordingly create the discrete grids in the curvelet domain. Note that the spatial and time steps are scale dependent.

2. Solve eq. (42) using numerical method in the curvelet domain. High accuracy numerical method is recommended for the estimation of the derivatives.

3. Apply the inverse curvelet transform to the final calculated curvelet coefficients $C_{i,j,k}$. We can also apply the curvelet transform to the data for some specific scales and directions to get a multi-scale and multi-direction view.

In our example, the grid size for u is 256 × 256, and the step size 10 m. The medium velocity is 1500 m/s and the main frequency of the ricker is 30 Hz. The curvelet transform is applied by the wrapping method and we have coarse scale, detailed scale and fine scale. For coarse scale, the time step is 0.1 ms. In the coarse domain, the equation is solved by central difference method and in the detailed and fine scale, pseudospectral method is used for high accuracy.

Fig. 2 displays the snapshots of the wave field at the time t = 2.0 s in the coarse and detail scale. Fig. 3 shows the snapshots of every direction in the detail scale. For individual snapshots, we only use the coefficients in one direction and then apply the inverse curvelet transform. As the figure shows, the total wavefield is composed of the waves in different directions.

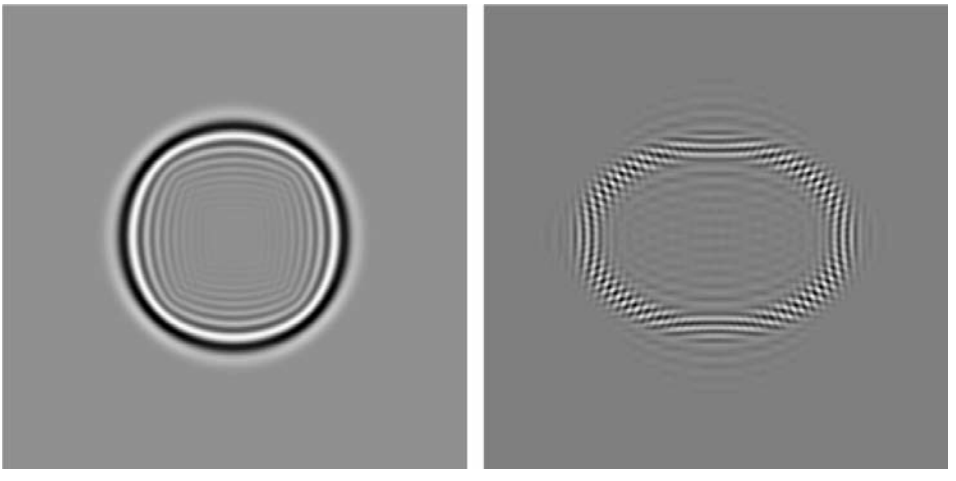

Fig. 2. Snapshot of the wave field in the coarse and detail scale.

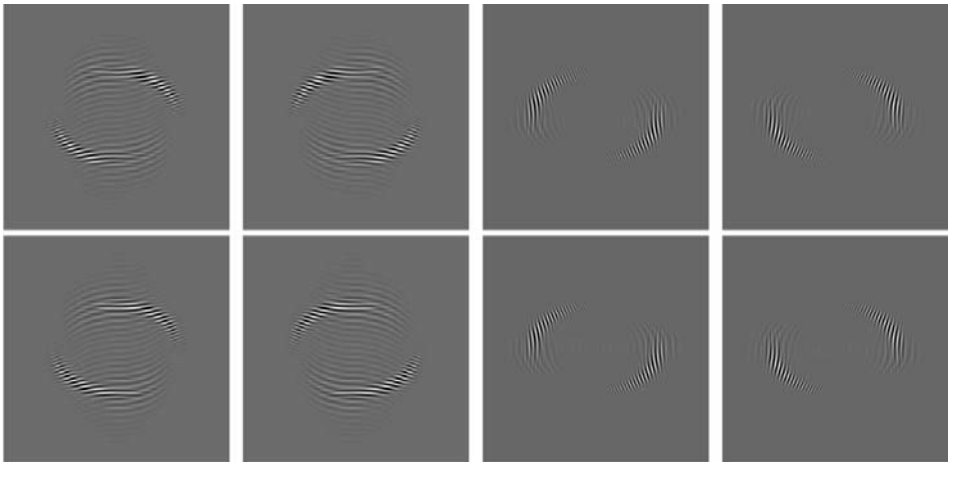

Fig. 3. Snapshot of the wave field in the detail scale for eight different directions.

Fig. 4 shows that the wave field evolves in certain scale and direction. From top-bottom and right to left, the corresponding time starts from 10 ms, every 10 ms until 160 ms. We can see how the curvelet evolves in the spatial domain. At first, the wave field is composed of several curvelets, and then such curvelets appears to split and gradually form the wave front.

Numerical results acclaim the advantages of our method: first,we can get a multi-scale analysis of the wave motion as for wavelets. By comparison, the wave field can propagate in the coarse, detailed and fine scale, it appears that the energy is much focused in the coarse scale. On the other hand, we can also obtain a multi-directional analysis of the wave motion. Using the curvelets, we

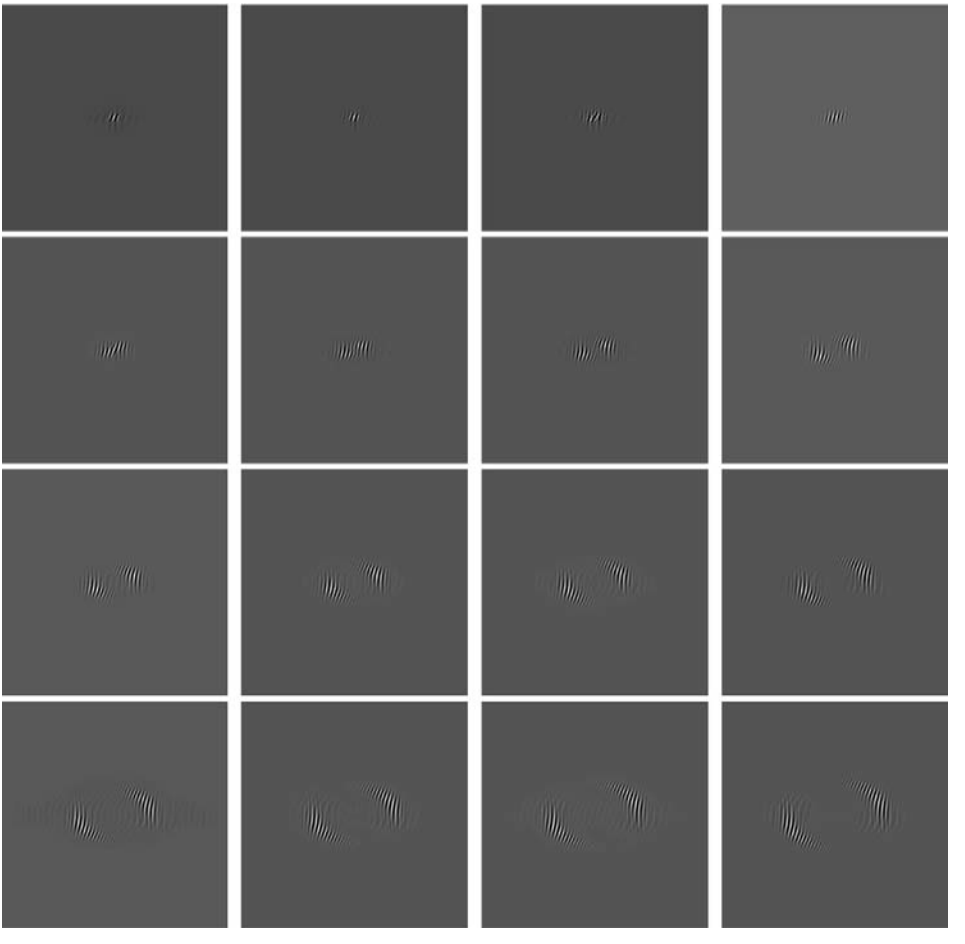

Fig. 4. Evolution of the wave field in the detail scale, from 10 ms every 10 ms until 160 ms.

have a multi-direction view of the wave propagation as the petal-like image in Fig. 3. This has a potential application for wave modeling in certain direction, because we can ignore unimportant directions and this will sufficiently reduce the computation time and storage space.

In the section on curvelets, we have presented the derivatives of arbitrary functions in the curvelet domain. We can easily extend the strategy to other linear partial differential equations with constant coefficients. For example, the 2D homogeneous elastic wave equation in the curvelet domain is:

$$\rho(\partial^2 C^u_{j,l,k}/\partial t^2 = (\lambda + \mu)[(\partial^2 C^u_{j,l,k}/\partial b_1^2) - \tan\theta_l(\partial^2 C^v_{j,l,k}/\partial b_1^2) + (\partial^2 C^v_{j,l,k}/\partial b_1 \partial b_2)]$$

$$+ \mu[(1 + \tan^2\theta_l)(\partial^2 C^u_{j,l,k}/\partial b_1^2) + (\partial^2 C^u_{j,l,k}/\partial b_2^2) - 2\tan\theta_l(\partial^2 C^u_{j,l,k}/\partial b_1 \partial b_2)] \quad , \quad (43)$$

$$\rho(\partial^2 C^v_{j,l,k}/\partial t^2 = (\lambda + \mu)[(\partial^2 C^v_{j,l,k}/\partial b_1^2) - \tan\theta_l(\partial^2 C^u_{j,l,k}/\partial b_1^2) + (\partial^2 C^u_{j,l,k}/\partial b_1 \partial b_2)]$$

$$+ \mu[(1 + \tan^2\theta_l)(\partial^2 C^v_{j,l,k}/\partial b_1^2) + (\partial^2 C^v_{j,l,k}/\partial b_2^2) - 2\tan\theta_l(\partial^2 C^v_{j,l,k}/\partial b_1 \partial b_2)] \quad , \quad (44)$$

where λ, μ are the Lamé constants, ρ the density. $C^u_{j,l,k}$, $C^v_{j,l,k}$ represent the curvelet transform of the displacement u and v.

For heterogeneous media, following the principle of section on curvelets, the Laplacian of the pressure field u can be decomposed into a sum of curvelets (3 terms). If a depends on x, then we must calculate the following coefficients $a_{j,l,k,m,n,q}$:

$$a_{j,l,k,m,n,q} = \int a^2(x)\varphi_{m,n,q}(x)\varphi_{j,l,k}(x)dx \quad , \quad (45)$$

and the wave equation in the curvelet domain changes to

$$\partial^2 C_{j,l,k}/\partial t^2 = \sum_{m,n,q} \{a_{j,l,k,m,n,q}[(1 + \tan^2\theta_l)(\partial^2 C_{j,l,k}/\partial b_1^2) + (\partial^2 C_{j,l,k}/\partial b_2^2)$$

$$- 2\tan\theta_l(\partial^2 C_{j,l,k}/\partial b_1 \partial b_2]\} \quad . \quad (46)$$

Calculation of eq. (45) would be a key issue in numerical simulation of heterogeneous model. This would be included in our future research.

CONCLUSION

This paper is a first attempt towards solving the wave equation in the curvelet domain. We have derived an expression for homogeneous velocity models. For the extension to more complex models, the expression obtained here of the spatial derivatives in the curvelet domain remains true. More work is however needed to establish the final formulation.

REFERENCES

Alford, R.M., Kelly, K.R. and Boore, D.M., 1974. Accuracy of finite difference modeling of the acoustic wave equation. Geophysics, 39: 834-842.

Alterman, Z. and Karal, F.C., 1968. Propagation of elastic waves in layered media by finite difference methods. Bull. Seismol. Soc. Am, 58: 367-398.

Andersson, F., de Hoop, M.V., Smith, H. and Uhlmann, G., 2003. A multi-scale approach to hyperbolic evolution equations with limited smoothness communications in partial differential equations. C.R. Acad. Sci. Paris, 33: 988-1017.

Antoine, J.P., Murenzi, R., Vandergheynst, P. and Ali, S.T., 2004. Two-dimensional wavelets and their relatives. Cambridge University Press, Cambridge.

Candès, E.J. and Demanet, L., 2005. The curvelet representation of wave propagators is optimally sparse. Comm. Pure Appl. Math., 58: 1472-1528.

Candès, E.J. and Donoho, D.L., 2000, Curvelet a surprisingly effective nonadaptive representation for objects with edges. Curves and Surfaces, Vanderbilt University Press: 105-120.

Candès, E.J. and Donoho, D.L., 2003. Curvelets and Fourier Integral Operators. C.R. Acad. Sci. Paris, 1: 395-398.

Candès, E.J. and Donoho, D.L., 2004. New tight frames of curvelets and optimal representations of objects with piecewise C^2 singularities. Comm. Pure Appl. Math., 57: 219-266.

Candès, E.J., Demanet, L., Donoho, D.L. and Ying, L., 2005. Fast discrete curvelet transforms. Multiscale. Model. Simul., 5: 861-899.

Carrer, J., Mansur, W. and Vanzuit, R., 2008. Scalar wave equation by the boundary element method: a D-BEM approach with non-homogeneous initial conditions. Computat. Mechan., 44: 31-44.

Chauris, H. and Nguyen, T.T., 2008. Seismic demigration/migration in the curvelet domain. Geophysics, 73: 35-46.

Daubechies, I., 1992. Ten Lectures on Wavelets. SIAM, Philadelphia.

Demanet, L., 2006. Curvelets, Wave Atoms and Wave Equations. Ph.D. Thesis, California Institute of Technology, Pasadena.

Douma, H. and de Hoop, M.V., 2007. Leading-order seismic imaging using curvelets. Geophysics, 72: 231-248.

Fornberg, B., 1989. Pseudospectral approximation of the elastic wave equation on staggered grid. Expanded Abstr., 59th Ann. Internat. SEG Mtg., Dallas, 8: 1047-1049.

Funato, K. and Fukui, T., 1999. Time domain boundary element method for wave propagation in biot material. Proc. Japan Nat. Symp. Boundary Element Meth., 16: 7-12.

Gazdag, J., 1981. Modeling of the acoustic wave equation with transform methods. Geophysics, 46: 854-859.

Herrmann, F.J., Wang, D., Hennenfent, G. and Moghaddam, P.P., 2008. Curvelet-based seismic data processing: A multiscale and nonlinear approach. Geophysics, 73: A1-A5.

Hong, T.K. and Kennett, B.L., 2002a, A wavelet based method for simulation of two-dimensional elastic wave propagation. Geophys. J. Internat., 150: 610-638.

Hong, T.K. and Kennett, B.L., 2002b. A wavelet based method for the numerical simulation of wave propagation. J. Comput. Phys., 183, 577-622.

Kelly, K., Ward, R. and Treitel, S., 1976. Synthetic seismograms: a finite-difference approach. Geophysics, 41: 2-27.

Kosloff, D. and Baysal, E., 1982. Forward modeling by a Fourier method. Geophysics, 47: 1402-1412.

Lin, T. and Herrmann, F.J., 2007. Compressed wavefield extrapolation. Geophysics, 72: SM77-SM93.

Lysmer, J. and Draker, L., 1972. A finite element method for seismology in methods in computational physics, Vol. 11. Academic Press, New York.

Ma, J., Gang, T. and Hussaini, M., 2007. A refining estimation for adaptive solution of wave equation based on curvelets. Proc. SPIE, San Diego: 67012J.

Ma, J. and Plonka, G., 2007. Combined curvelet shrinkage and nonlinear anisotropic diffusion. IEEE Trasnsact. Image Process., 16: 2198-2206.

Ma, J. and Plonka, G., 2009a. Computing with curvelets: from imaging processing to turbulent flows. IEEE J. Comput. Sci. Eng., 11: 72-80.

Ma, J. and Plonka, G., 2009b. A review of curvelets and recent applications. IEEE Signal Process. Magaz., in press.

Ma, J., Yang, H. and Zhu, Y., 2001. MRFD method for numerical solution of wave propagation in layered media with general boundary condition. Electron. Lett., 37: 1267-1268.

Meyer, Y., 1992. Wavelet and Operators. Cambridge University Press, Cambridge.

Mullen, R. and Belytschko, T., 1982. Dispersion analysis of finite element semidiscretizations of the two-dimensional wave equation. Internat. J. Numerical Methods in Engin., 18: 11-29.